Boulder Summer School 2008.

HEAVY FERMIONS: ELECTRONS AT THE EDGE OF MAGNETISM II

Lecture Notes II.
Piers Coleman.

1. Anderson Model
2. Adiabaticity and the Kondo Resonance
3. Renormalization concept
4. Schrieffer Wolff transformation
5. Kondo Effect
6. Universality in the Kondo Effect
7. Doniach's Kondo Lattice Concept

2 LOCAL MOMENTS AND THE KONDO LATTICE

2.1 Local moment formation

2.1.1 The Anderson model

We begin with a discussion of how magnetic moments form at high temperatures, and how they are screened again at low temperatures to form a Fermi liquid. The basic model for local moment formation is the Anderson model (Anderson, 1961)

$$H = \overbrace{\sum_{k,\sigma} \epsilon_k n_{k\sigma} + \sum_{k,\sigma} V(k)\left[c^\dagger_{k\sigma} f_\sigma + f^\dagger_\sigma c_{k\sigma}\right]}^{H_{\rm resonance}} + \underbrace{E_{\rm f} n_{\rm f} + U n_{{\rm f}\uparrow} n_{{\rm f}\downarrow}}_{H_{\rm atomic}} \tag{21}$$

where $H_{\rm atomic}$ describes the atomic limit of an isolated magnetic ion and $H_{\rm resonance}$ describes the hybridization of the localized f electrons in the ion with the Bloch waves of the conduction sea. For pedagogical reasons, our discussion initially focuses on the case where the f state is a Kramer's doublet.

There are two key elements to the Anderson model:

- *Atomic limit:* The atomic physics of an isolated ion with a single f state, described by the model

$$H_{\rm atomic} = E_f n_f + U n_{f\uparrow} n_{f\downarrow} \tag{22}$$

Here E_f is the energy of the f state and U is the Coulomb energy associated with two electrons in the same orbital. The atomic physics contains the basic mechanism for local moment formation, valid for f electrons, but also seen in a variety of other contexts, such as transition-metal atoms and quantum dots.
The four quantum states of the atomic model are

$$\left.\begin{array}{ll} |f^2\rangle & E(f^2) = 2E_f + U \\ |f^0\rangle & E(f^0) = 0 \end{array}\right\}\text{nonmagnetic}$$
$$|f^1\uparrow\rangle\ |f^1\downarrow\rangle\ \ E(f^1) = E_f \qquad \text{magnetic} \tag{23}$$

In a magnetic ground state, the cost of inducing a 'valence fluctuation' by removing or adding an electron to the f^1 state is positive, that is,

$$\text{removing:} \quad E(f^0) - E(f^1) = -E_f > 0 \Rightarrow \frac{U}{2} > E_f + \frac{U}{2} \tag{24}$$

$$\text{adding:} \quad E(f^2) - E(f^1) = E_f + U > 0 \Rightarrow E_f + \frac{U}{2} > -\frac{U}{2} \tag{25}$$

or (Figure 10).

$$\frac{U}{2} > E_f + \frac{U}{2} > -\frac{U}{2} \tag{26}$$

Under these conditions, a local moment is well defined, provided the temperature is lower than the valence fluctuation scale $T_{\rm VF} = \max(E_{\rm f} + U, -E_{\rm f})$. At lower temperatures, the atom behaves exclusively as a quantum top.

- *Virtual bound-state formation.* When the magnetic ion is immersed in a sea of electrons, the f electrons within the core of the atom hybridize with the Bloch states of surrounding electron sea (Blandin and Friedel, 1958) to form a resonance described by

$$H_{\rm resonance} = \sum_{k,\sigma} \epsilon_k n_{k\sigma} + \sum_{k,\sigma} \left[V(\mathbf{k}) c^\dagger_{k\sigma} f_\sigma + V(\mathbf{k})^* f^\dagger_\sigma c_{k\sigma} \right] \tag{27}$$

where the hybridization matrix element $V(\mathbf{k}) = \langle \mathbf{k} | V_{\rm atomic} | f \rangle$ is the overlap of the atomic potential between a localized f state and a Bloch wave. In the absence of any interactions, the hybridization broadens the localized f state, producing a resonance of width

$$\Delta = \pi \sum_{\mathbf{k}} |V(\mathbf{k})|^2 \delta(\epsilon_{\mathbf{k}} - \mu) = \pi V^2 \rho \tag{28}$$

where V^2 is the average of the hybridization around the Fermi surface.

There are two complementary ways to approach the physics of the Anderson model:

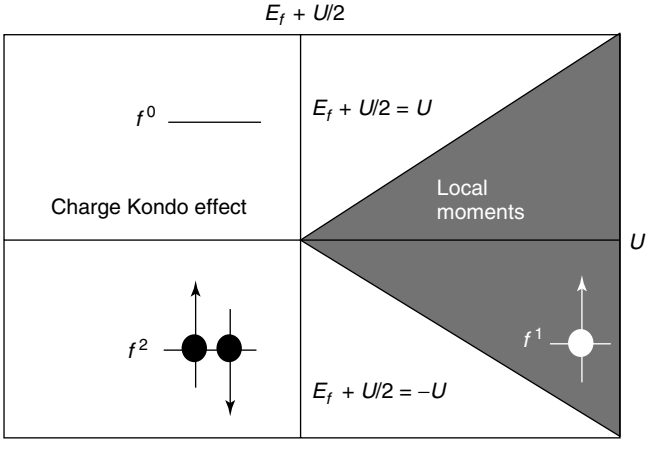

Figure 10. Phase diagram for Anderson impurity model in the atomic limit.

- The 'atomic picture', which starts with the interacting, but isolated atom ($V(k) = 0$), and considers the effect of immersing it in an electron sea by slowly dialing up the hybridization.
- The 'adiabatic picture', which starts with the noninteracting resonant ground state ($U = 0$), and then considers the effect of dialing up the interaction term U.

These approaches paint a contrasting and, at first sight, contradictory picture of a local moment in a Fermi sea. From the adiabatic perspective, the ground state is always a Fermi liquid (see 1.2.2), but from atomic perspective, provided the hybridization is smaller than U, one expects a local magnetic moment, whose low-lying degrees of freedom are purely rotational. How do we resolve this paradox?

Anderson's original work provided a mean-field treatment of the interaction. He found that at interactions larger than $U_c \sim \pi\Delta$ local moments develop with a finite magnetization $M = \langle n_\uparrow \rangle - \langle n_\downarrow \rangle$. The mean-field theory provides an approximate guide to the conditions required for moment formation, but it does not account for the restoration of the singlet symmetry of the ground state at low temperatures. The resolution of the adiabatic and the atomic picture derives from quantum spin fluctuations, which cause the local moment to 'tunnel' on a slow timescale τ_{sf} between the two degenerate 'up' and 'down' configurations.

$$e^-_\downarrow + f^1_\uparrow \rightleftharpoons e^-_\uparrow + f^1_\downarrow \tag{29}$$

These fluctuations are the origin of the Kondo effect. From the energy uncertainty principle, below a temperature $T_{\rm K}$, at which the thermal excitation energy $k_{\rm B}T$ is of the order of the characteristic tunneling rate $\frac{\hbar}{\tau_{sf}}$, a paramagnetic state with a Fermi-liquid resonance forms. The characteristic width of the resonance is then determined by the Kondo energy $k_{\rm B}T_{\rm K} \sim \frac{\hbar}{\tau_{sf}}$. The existence of this resonance was first deduced by Abrikosov (1965), and Suhl (1965), but it is more frequently called the *Kondo resonance*. From perturbative renormalization group reasoning (Haldane, 1978) and the Bethe Ansatz solution of the Anderson model (Wiegmann, 1980; Okiji and Kawakami, 1983), we know that, for large $U \gg \Delta$, the Kondo scale depends exponentially on U. In the symmetric Anderson model, where $E_f = -U/2$,

$$T_K = \sqrt{\frac{2U\Delta}{\pi^2}} \exp\left(-\frac{\pi U}{8\Delta}\right) \tag{30}$$

The temperature $T_{\rm K}$ marks the crossover from a a high-temperature Curie-law $\chi \sim \frac{1}{T}$ susceptibility to a low-temperature paramagnetic susceptibility $\chi \sim 1/T_{\rm K}$.

2.1.2 Adiabaticity and the Kondo resonance

A central quantity in the physics of f-electron systems is the f-spectral function,

$$A_f(\omega) = \frac{1}{\pi}\mathrm{Im}G_f(\omega - i\delta) \tag{31}$$

where $G_f(\omega) = -i\int_{-\infty}^{\infty} \mathrm{d}t\langle \mathrm{T} f_\sigma(t) f_\sigma^\dagger(0)\rangle \mathrm{e}^{i\omega t}$ is the Fourier transform of the time-ordered f-Green's function. When an f electron is added, or removed from the f state, the final state has a distribution of energies described by the f-spectral function. From a spectral decomposition of the f-Green's function, the positive energy part of the f-spectral function determines the energy distribution for electron addition, while the negative energy part measures the energy distribution of electron removal:

$$A_f(\omega) = \begin{cases} \overbrace{\sum_\lambda \left|\langle\lambda| f_\sigma^\dagger |\phi_0\rangle\right|^2 \delta(\omega - [E_\lambda - E_0]),}^{\text{Energy distribution of state formed by adding one f electron}} & (\omega > 0) \\ \underbrace{\sum_\lambda \left|\langle\lambda| f_\sigma |\phi_0\rangle\right|^2 \delta(\omega - [E_0 - E_\lambda]),}_{\text{Energy distribution of state formed by removing an f electron}} & (\omega < 0) \end{cases} \tag{32}$$

where E_0 is the energy of the ground state, and E_λ is the energy of an excited state λ, formed by adding or removing an f electron. For negative energies, this spectrum can be measured by measuring the energy distribution of photoelectrons produced by X-ray photoemission, while for positive energies, the spectral function can be measured from inverse X-ray photoemission (Allen *et al.*, 1986; Allen, Oh, Maple and Torikachvili, 1983). The weight beneath the Fermi energy peak determines the f charge of the ion

$$\langle n_f\rangle = 2\int_{-\infty}^{0} \mathrm{d}\omega A_f(\omega) \tag{33}$$

In a magnetic ion, such as a Cerium atom in a $4f^1$ state, this quantity is just a little below unity.

Figure 11 illustrates the effect of the interaction on the f-spectral function. In the noninteracting limit ($U = 0$), the f-spectral function is a Lorentzian of width Δ. If we turn on the interaction U, being careful to shifting the f-level position beneath the Fermi energy to maintain a constant occupancy, the resonance splits into three peaks, two at energies $\omega = E_f$ and $\omega = E_f + U$ corresponding to the energies for a valence fluctuation, plus an additional central 'Kondo resonance' associated with the spin fluctuations of the local moment.

At first sight, once the interaction is much larger than the hybridization width Δ, one might expect there to be no spectral weight left at low energies. But this violates the idea of adiabaticity. In fact, there are always certain adiabatic

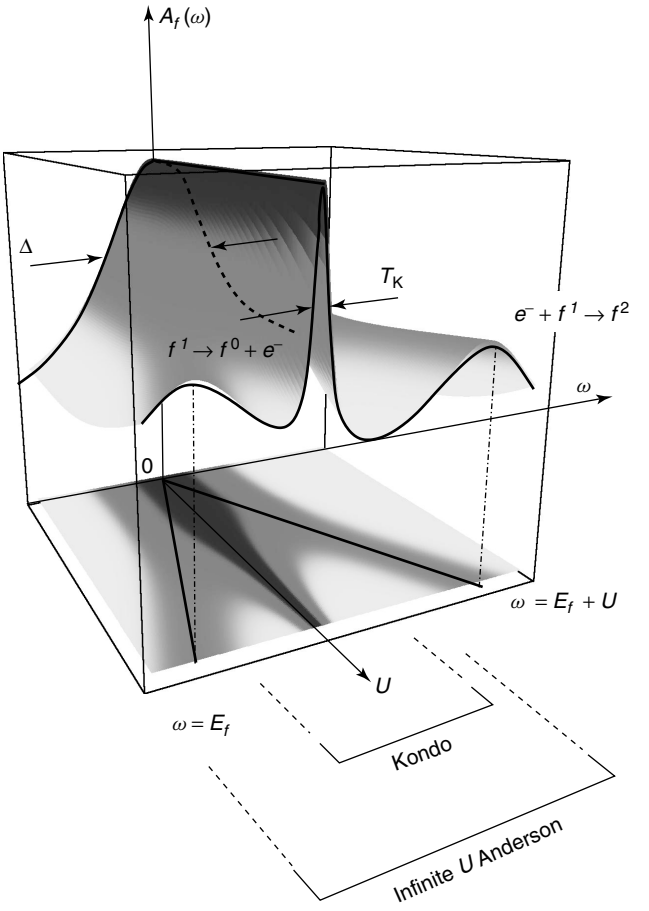

Figure 11. Schematic illustration of the evaluation of the f-spectral function $A_f(\omega)$ as interaction strength U is turned on continuously, maintaining a constant f occupancy by shifting the bare f-level position beneath the Fermi energy. The lower part of diagram is the density plot of f-spectral function, showing how the noninteracting resonance at $U = 0$ splits into an upper and lower atomic peak at $\omega = E_f$ and $\omega = E_f + U$.

invariants that do not change, despite the interaction. One such quantity is the phase shift δ_f associated with the scattering of conduction electrons of the ion; another is the height of the f-spectral function at zero energy, and it turns out that these two quantities are related. A rigorous result owing to (Langreth, 1966) tells us that the spectral function at $\omega = 0$ is directly determined by the f-phase shift, so that its noninteracting value

$$A_f(\omega = 0) = \frac{\sin^2\delta_f}{\pi\Delta} \tag{34}$$

is preserved by adiabaticity. Langreth's result can be heuristically derived by noting that δ_f is the phase of the f-Green's function at the Fermi energy, so that $G_f(0 - i\epsilon)^{-1} = |G_f^{-1}(0)|e^{-i\delta_f}$. Now, in a Fermi liquid, the scattering at the Fermi energy is purely elastic, and this implies

that $ImG_f^{-1}(0-i\epsilon)=\Delta$, the bare hybridization width. From this, it follows that $ImG_f^{-1}(0)=|G_f^{-1}(0)|\sin\delta_f=\Delta$, so that $G_f(0)=e^{i\delta_f}/(\Delta\sin\delta_f)$, and the preceding result follows.

The phase shift δ_f is set via the Friedel sum rule, according to which the sum of the up-and-down scattering phase shifts, gives the total number of f-bound electrons, or

$$\sum_\sigma \frac{\delta_{f\sigma}}{\pi}=2\frac{\delta_f}{\pi}=n_f \tag{35}$$

for a twofold degenerate f state. At large distances, the wave function of scattered electrons $\psi_f(r)\sim\sin(k_{\mathrm{F}}r+\delta_f)/r$ is 'shifted inwards' by a distance $\delta_l/k_{\mathrm{F}}=(\lambda_{\mathrm{F}}/2)\times(\delta_l/\pi)$. This sum rule is sometimes called a *node counting* rule because, if you think about a large sphere enclosing the impurity, then each time the phase shift passes through π, a node crosses the spherical boundary and one more electron per channel is bound beneath the Fermi sea. Friedel's sum rule holds for interacting electrons, provided the ground state is adiabatically accessible from the noninteracting system (Langer and Ambegaokar, 1961; Langreth, 1966). Since $n_f=1$ in an f^1 state, the Friedel sum rule tells us that the phase shift is $\pi/2$ for a twofold degenerate f state. In other words, adiabaticity tell us that the electron is *resonantly scattered* by the quenched local moment.

Photoemission studies do reveal the three-peaked structure characteristic of the Anderson model in many Ce systems, such as $CeIr_2$ and $CeRu_2$ (Allen, Oh, Maple and Torikachvili, 1983) (see Figure 12). Materials in which the Kondo resonance is wide enough to be resolved are more 'mixed valent' materials in which the f valence departs significantly from unity. Three-peaked structures have also been observed in certain U 5f materials such as UPt_3 and UAl_2 (Allen *et al.*, 1985) materials, but it has not yet been resolved in UBe_{13}. A three-peaked structure has recently been observed in 4f Yb materials, such as $YbPd_3$, where the $4f^{13}$ configuration contains a single f hole, so that the positions of the three peaks are reversed relative to Ce (Liu *et al.*, 1992).

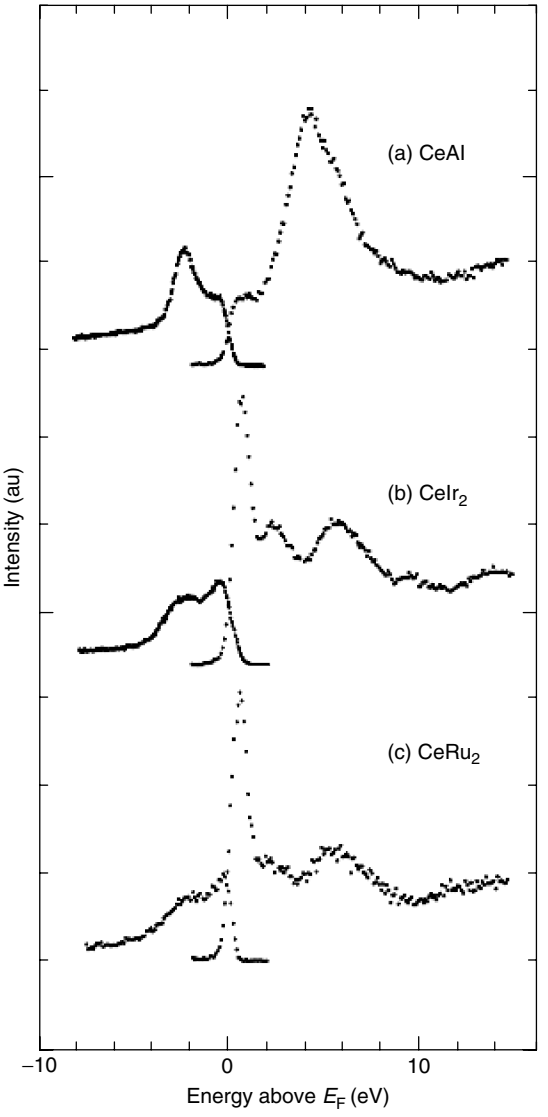

Figure 12. Showing spectral functions for three different Cerium f-electron materials, measured using X-ray photoemission (below the Fermi energy) and inverse X-ray photoemission (above the Fermi energy). CeAl is an AFM and does not display a Kondo resonance. (Reproduced from J.W. Allen, S.J. Oh, M.B. Maple and M.S. Torikachvili: *Phys. Rev.* **28**, 1983, 5347, copyright © 1983 by the American Physical Society, with permission of the APS.)

2.2 Hierarchies of energy scales

2.2.1 Renormalization concept

To understand how a Fermi liquid emerges when a local moment is immersed in a quantum sea of electrons, theorists had to connect physics on several widely spaced energy scales. Photoemission shows that the characteristic energy to produce a valence fluctuation is of the order of volts, or tens of thousands of Kelvin, yet the characteristic physics we are interested in occurs at scales hundreds or thousands of times smaller. How can we distill the essential effects of the atomic physics at electron volt scales on the low-energy physics at millivolt scales?

The essential tool for this task is the 'renormalization group' (Anderson and Yuval, 1969, 1970, 1971; Anderson, 1970, 1973; Wilson, 1976; Nozières and Blandin, 1980; Nozières, 1976), based on the idea that the physics at low-energy scales only depends on a small subset of 'relevant' variables from the original microscopic Hamiltonian. The extraction of these relevant variables is accomplished by

'renormalizing' the Hamiltonian by systematically eliminating the high-energy virtual excitations and adjusting the low-energy Hamiltonian to take care of the interactions that these virtual excitations induce in the low energy Hilbert space. This leads to a family of Hamiltonian's $H(\Lambda)$, each with a different high-energy cutoff Λ, which share the same low-energy physics.

The systematic passage from a Hamiltonian $H(\Lambda)$ to a renormalized Hamiltonian $H(\Lambda')$ with a smaller cutoff $\Lambda' = \Lambda/b$ is accomplished by dividing the eigenstates of H into a a low-energy subspace {L} and a high-energy subspace {H}, with energies $|\epsilon| < \Lambda' = \Lambda/b$ and a $|\epsilon| \in [\Lambda', \Lambda]$ respectively. The Hamiltonian is then broken up into terms that are block-diagonal in these subspaces,

$$H = \left[\begin{array}{c|c} H_{\rm L} & V^\dagger \\ \hline V & H_{\rm H} \end{array}\right] \tag{36}$$

where V and $V^\dagger$ provide the matrix elements between {L} and {H}. The effects of the V are then taken into account by carrying out a unitary (canonical) transformation that block-diagonalizes the Hamiltonian,

$$H(\Lambda) \to U H(\Lambda) U^\dagger = \left[\begin{array}{c|c} \tilde{H}_{\rm L} & 0 \\ \hline 0 & \tilde{H}_{\rm H} \end{array}\right] \tag{37}$$

The renormalized Hamiltonian is then given by $H(\Lambda') = \tilde{H}_{\rm L} = H_{\rm L} + \delta H$. The flow of key parameters in the Hamiltonian resulting from this process is called a *renormalization group flow*.

At certain important crossover energy scales, large tracts of the Hilbert space associated with the Hamiltonian are projected out by the renormalization process, and the character of the Hamiltonian changes qualitatively. In the Anderson model, there are three such important energy scales, (Figure 13)

- $\Lambda_I = E_f + U$, where valence fluctuations $e^- + f^1 \rightleftharpoons f^2$ into the doubly occupied f^2 state are eliminated. For $\Lambda \ll \Lambda_I$, the physics is described by the infinite U Anderson model

$$H = \sum_{k,\sigma} \epsilon_k n_{k\sigma} + \sum_{k,\sigma} V(k)\left[c^\dagger_{k\sigma} X_{0\sigma} + X_{\sigma 0} c_{k\sigma}\right] + E_f \sum_\sigma X_{\sigma\sigma}, \tag{38}$$

  where $X_{\sigma\sigma} = |f^1:\sigma\rangle\langle f^1:\sigma|$, $X_{0\sigma} = |f^0\rangle\langle f^1\sigma|$ and $X_{\sigma 0} = |f^1:\sigma\rangle\langle f^0|$ are 'Hubbard operators' that connect the states in the projected Hilbert space with no double occupancy.
- $\Lambda_{II} \sim |E_f| = -E_f$, where valence fluctuations into the empty state $f^1 \rightleftharpoons f^0 + e^-$ are eliminated to form a local moment. Physics below this scale is described by the Kondo model.
- $\Lambda = T_{\rm K}$, the Kondo temperature below which the local moment is screened to form a resonantly scattering local Fermi liquid.

In the symmetric Anderson model, $\Lambda_I = \Lambda_{II}$, and the transition to local moment behavior occurs in a one-step crossover process.

2.2.2 *Schrieffer–Wolff transformation*

The unitary or canonical transformation that eliminates the charge fluctuations at scales Λ_I and Λ_{II} was first

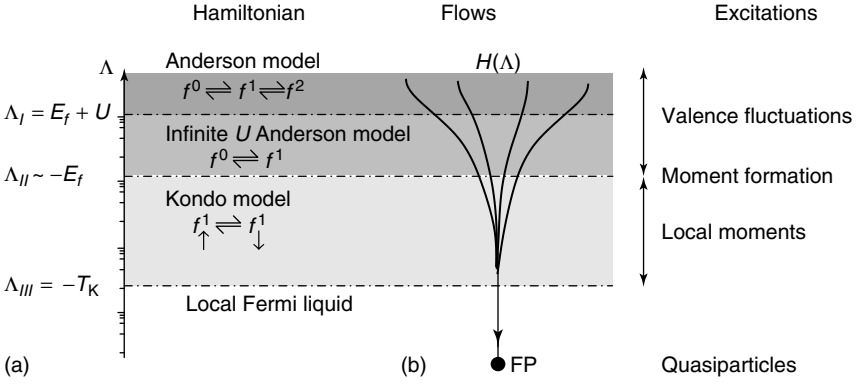

Figure 13. (a) Crossover energy scales for the Anderson model. At scales below Λ_I, valence fluctuations into the doubly occupied state are suppressed. All lower energy physics is described by the infinite U Anderson model. Below Λ_{II}, all valence fluctuations are suppressed, and the physics involves purely the spin degrees of freedom of the ion, coupled to the conduction sea via the Kondo interaction. The Kondo scale renormalizes to strong coupling below Λ_{III}, and the local moment becomes screened to form a local Fermi liquid. (b) Illustrating the idea of renormalization group flows toward a Fermi liquid fixed point.

carried out by Schrieffer and Wolff (1966), and Coqblin and Schrieffer (1969), who showed how this model gives rise to a residual antiferromagnetic interaction between the local moment and conduction electrons. The emergence of this antiferromagnetic interaction is associated with a process called *superexchange*: the virtual process in which an electron or hole briefly migrates off the ion, to be immediately replaced by another with a different spin. When these processes are removed by the canonical transformation, they induce an antiferromagnetic interaction between the local moment and the conduction electrons. This can be seen by considering the two possible spin-exchange processes

$$\begin{aligned} e^-_\uparrow + f^1_\downarrow &\leftrightarrow f^2 \leftrightarrow e^-_\downarrow + f^1_\uparrow \qquad \Delta E_I \sim U + E_f \\ h^+_\uparrow + f^1_\downarrow &\leftrightarrow f^0 \leftrightarrow h^+_\downarrow + f^1_\uparrow \qquad \Delta E_{II} \sim -E_f \end{aligned} \tag{39}$$

Both processes require that the f electron and incoming particle are in a spin-singlet. From second-order perturbation theory, the energy of the singlet is lowered by an amount $-2J$, where

$$J = V^2 \left[\frac{1}{\Delta E_1} + \frac{1}{\Delta E_2} \right] \tag{40}$$

and the factor of two derives from the two ways a singlet can emit an electron or hole into the continuum [1] and $V \sim V(k_{\rm F})$ is the hybridization matrix element near the Fermi surface. For the symmetric Anderson model, where $\Delta E_1 = \Delta E_{II} = U/2$, $J = 4V^2/U$.

If we introduce the electron spin-density operator $\vec{\sigma}(0) = \frac{1}{\mathcal{N}} \sum_{k,k'} c^\dagger_{k\alpha} \vec{\sigma}_{\alpha\beta} c_{k'\beta}$, where $\mathcal{N}$ is the number of sites in the lattice, then the effective interaction has the form

$$H_{\rm K} = -2J P_{S=0} \tag{41}$$

where $P_{S=0} = \left[\frac{1}{4} - \frac{1}{2} \vec{\sigma}(0) \cdot \vec{S}_f \right]$ is the singlet projection operator. If we drop the constant term, then the effective interaction induced by the virtual charge fluctuations must have the form

$$H_{\rm K} = J \vec{\sigma}(0) \cdot \vec{S}_f \tag{42}$$

where $\vec{S}_f$ is the spin of the localized moment. The complete 'Kondo Model', $H = H_c + H_{\rm K}$ describing the conduction electrons and their interaction with the local moment is

$$H = \sum_{\mathbf{k}\sigma} \epsilon_{\mathbf{k}} c^\dagger_{\vec{k}\sigma} c_{\vec{k}\sigma} + J \vec{\sigma}(0) \cdot \vec{S}_f \tag{43}$$

2.2.3 The Kondo effect

The antiferromagnetic sign of the superexchange interaction J in the Kondo Hamiltonian is the origin of the spin-screening physics of the Kondo effect. The bare interaction is weak, but the spin fluctuations it induces have the effect of *antiscreening* the interaction at low energies, renormalizing it to larger and larger values. To see this, we follow an Anderson's 'Poor Man's' scaling procedure (Anderson, 1973, 1970), which takes advantage of the observation that at small J the renormalization in the Hamiltonian associated with the block-diagonalization process $\delta H = \tilde{H}_{\rm L} - H_{\rm L}$ is given by second-order perturbation theory:

$$\delta H_{ab} = \langle a | \delta H | b \rangle = \frac{1}{2} \left[T_{ab}(E_a) + T_{ab}(E_b) \right] \tag{44}$$

where

$$T_{ab}(\omega) = \sum_{|\Lambda\rangle \in \{H\}} \left[\frac{V^\dagger_{a\Lambda} V_{\Lambda b}}{\omega - E_\Lambda} \right] \tag{45}$$

is the many-body 't-matrix' associated with virtual transitions into the high-energy subspace $\{H\}$. For the Kondo model,

$$V = \mathcal{P}_{\rm H} J \vec{S}(0) \cdot \vec{S}_d \mathcal{P}_{\rm L} \tag{46}$$

where $\mathcal{P}_{\rm H}$ projects the intermediate state into the high-energy subspace, while $\mathcal{P}_{\rm L}$ projects the initial state into the low-energy subspace. There are two virtual scattering processes that contribute to the antiscreening effect, involving a high-energy electron (I) or a high-energy hole (II).

Process I is denoted by the diagram

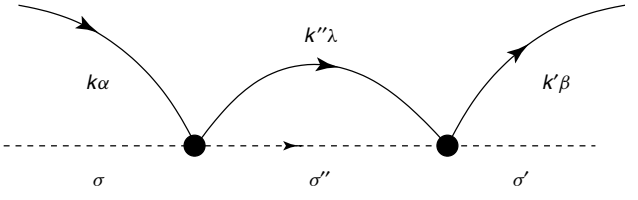

and starts in state $|b\rangle = |k\alpha, \sigma\rangle$, passes through a virtual state $|\Lambda\rangle = |c^\dagger_{k''} \alpha \sigma''\rangle$ where $\epsilon_{k''}$ lies at high energies in the range $\epsilon_{k''} \in [\Lambda/b, \Lambda]$ and ends in state $|a\rangle = |k'\beta, \sigma'\rangle$. The resulting renormalization

$$\begin{aligned} &\langle k'\beta, \sigma' | T^I(E) | k\alpha, \sigma \rangle \\ &\quad = \sum_{\epsilon_{k''} \in [\Lambda - \delta\Lambda, \Lambda]} \left[\frac{1}{E - \epsilon_{k''}} \right] J^2 \times (\sigma^a_{\beta\lambda} \sigma^b_{\lambda\alpha})(S^a_{\sigma'\sigma''} S^b_{\sigma''\sigma}) \\ &\quad \approx J^2 \rho \delta\Lambda \left[\frac{1}{E - \Lambda} \right] (\sigma^a \sigma^b)_{\beta\alpha} (S^a S^b)_{\sigma'\sigma} \end{aligned} \tag{47}$$

In *Process II*, denoted by

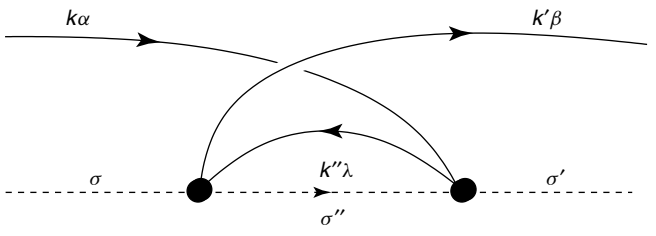

the formation of a virtual hole excitation $|\Lambda\rangle = c_{k''\lambda}|\sigma''\rangle$ introduces an electron line that crosses itself, introducing a negative sign into the scattering amplitude. The spin operators of the conduction sea and AFM reverse their relative order in process II, which introduces a relative minus sign into the T-matrix for scattering into a high-energy hole-state,

$$\begin{aligned}
&\langle k'\beta\sigma'|T^{(II)}(E)|k\alpha\sigma\rangle \\
&\quad = -\sum_{\epsilon_{k''}\in[-\Lambda,-\Lambda+\delta\Lambda]}\left[\frac{1}{E-(\epsilon_k+\epsilon_{k'}-\epsilon_{k''})}\right] \\
&\qquad \times J^2(\sigma^b\sigma^a)_{\beta\alpha}(S^aS^b)_{\sigma'\sigma} \\
&\quad = -J^2\rho\delta\Lambda\left[\frac{1}{E-\Lambda}\right](\sigma^a\sigma^b)_{\beta\alpha}(S^aS^b)_{\sigma'\sigma} \qquad (48)
\end{aligned}$$

where we have assumed that the energies ϵ_k and $\epsilon_{k'}$ are negligible compared with Λ.

Adding equations (47 and 48) gives

$$\begin{aligned}
\delta H^{int}_{k'\beta\sigma';k\alpha\sigma} &= \hat{T}^I + T^{II} = -\frac{J^2\rho\delta\Lambda}{\Lambda}[\sigma^a,\sigma^b]_{\beta\alpha}S^aS^b \\
&= 2\frac{J^2\rho\delta\Lambda}{\Lambda}\vec{\sigma}_{\beta\alpha}\cdot\vec{S}_{\sigma'\sigma} \qquad (49)
\end{aligned}$$

so the high-energy virtual spin fluctuations enhance or 'antiscreen' the Kondo coupling constant

$$J(\Lambda') = J(\Lambda) + 2J^2\rho\frac{\delta\Lambda}{\Lambda} \qquad (50)$$

If we introduce the coupling constant $g = \rho J$, recognizing that $d\ln\Lambda = -\frac{\delta\Lambda}{\Lambda}$, we see that it satisfies

$$\frac{\partial g}{\partial\ln\Lambda} = \beta(g) = -2g^2 + O(g^3) \qquad (51)$$

This is an example of a **negative** β function: a signature of an interaction that grows with the renormalization process. At high energies, the weakly coupled local moment is said to be **asymptotically free**. The solution to the scaling equation is

$$g(\Lambda') = \frac{g_o}{1-2g_o\ln(\Lambda/\Lambda')} \qquad (52)$$

and if we introduce the 'Kondo temperature'

$$T_{\rm K} = D\exp\left[-\frac{1}{2g_o}\right] \qquad (53)$$

we see that this can be written

$$2g(\Lambda') = \frac{1}{\ln(\Lambda/T_{\rm K})} \qquad (54)$$

so that once $\Lambda' \sim T_{\rm K}$, the coupling constant becomes of the order one – at lower energies, one reaches 'strong coupling' where the Kondo coupling can no longer be treated as a weak perturbation. One of the fascinating things about this flow to strong coupling is that, in the limit $T_{\rm K} \ll D$, all explicit dependence on the bandwidth D disappears and the Kondo temperature $T_{\rm K}$ is the only intrinsic energy scale in the physics. Any physical quantity must depend in a universal way on ratios of energy to $T_{\rm K}$, thus the universal part of the free energy must have the form

$$F(T) = T_{\rm K}\Phi\frac{T}{T_{\rm K}} \qquad (55)$$

where $\Phi(x)$ is universal. We can also understand the resistance created by spin-flip scattering of a magnetic impurity in the same way. The resistivity is given by $\rho_i = \frac{ne^2}{m}\tau(T,H)$, where the scattering rate must also have a scaling form

$$\tau(T,H) = \frac{n_i}{\rho}\Phi_2\left(\frac{T}{T_{\rm K}},\frac{H}{T_{\rm K}}\right) \qquad (56)$$

where ρ is the density of states (per spin) of electrons and n_i is the concentration of magnetic impurities and the function $\Phi_2(t,h)$ is universal. To leading order in the Born approximation, the scattering rate is given by $\tau = 2\pi\rho J^2S(S+1) = \frac{2\pi S(S+1)}{\rho}(g_0)^2$ where $g_0 = g(\Lambda_0)$ is the bare coupling at the energy scale that moments form. We can obtain the behavior at a finite temperature by replacing $g_0 \to g(\Lambda = 2\pi T)$, where upon

$$\tau(T) = \frac{2\pi S(S+1)}{\rho}\frac{1}{4\ln^2(2\pi T/T_{\rm K})} \qquad (57)$$

gives the leading high-temperature growth of the resistance associated with the Kondo effect.

The kind of perturbative analysis we have gone through here takes us down to the Kondo temperature. The physics at lower energies corresponds to the strong coupling limit of the Kondo model. Qualitatively, once $J\rho \gg 1$, the local moment is bound into a spin-singlet with a conduction electron. The number of bound electrons is $n_f = 1$, so that by the Friedel sum rule (equation (35)) in a paramagnet the phase shift $\delta_\uparrow = \delta_\downarrow = \pi/2$, the unitary limit of scattering. For more

details about the local Fermi liquid that forms, we refer the reader to the accompanying chapter on the Kondo effect by Jones (2007).

2.2.4 Doniach's Kondo lattice concept

The discovery of heavy-electron metals prompted Doniach (1977) to make the radical proposal that heavy-electron materials derive from a dense lattice version of the Kondo effect, described by the **Kondo Lattice model** (Kasuya, 1956)

$$H = \sum_{\mathbf{k}\sigma} \epsilon_{\mathbf{k}} c^{\dagger}_{\mathbf{k}\sigma} c_{\mathbf{k}\sigma} + J \sum_j \vec{S}_j \cdot c^{\dagger}_{\mathbf{k}\alpha} \vec{\sigma}_{\alpha\beta} c_{\mathbf{k}'\beta} \mathrm{e}^{i(\mathbf{k}'-\mathbf{k})\cdot\mathbf{R}_j} \tag{58}$$

In effect, Doniach was implicitly proposing that the key physics of heavy-electron materials resides in the interaction of neutral local moments with a charged conduction electron sea.

Most local moment systems develop an antiferromagnetic order at low temperatures. A magnetic moment at location $\mathbf{x}_0$ induces a wave of 'Friedel' oscillations in the electron spin density (Figure 14)

$$\langle \vec{\sigma}(\mathbf{x}) \rangle = -J\chi(\mathbf{x}-\mathbf{x}_0)\langle \vec{S}(\mathbf{x}_0) \rangle \tag{59}$$

where

$$\chi(\mathbf{x}) = 2\sum_{\mathbf{k},\mathbf{k}'} \left(\frac{f(\epsilon_{\mathbf{k}}) - f(\epsilon_{\mathbf{k}'})}{\epsilon_{\mathbf{k}'} - \epsilon_{\mathbf{k}}} \right) e^{i(\mathbf{k}-\mathbf{k}')\cdot\mathbf{x}} \tag{60}$$

is the nonlocal susceptibility of the metal. The sharp discontinuity in the occupancies $f(\epsilon_k)$ at the Fermi surface is responsible for Friedel oscillations in induced spin density that decay with a power law

$$\langle \vec{\sigma}(r) \rangle \sim -J\rho \frac{\cos 2k_{\mathrm{F}} r}{|k_{\mathrm{F}} r|^3} \tag{61}$$

where ρ is the conduction electron density of states and r is the distance from the impurity. If a second local moment is introduced at location $\mathbf{x}$, it couples to this Friedel oscillation with energy $J\langle \vec{S}(\mathbf{x}) \cdot \vec{\sigma}(x) \rangle$, giving rise to the 'RKKY' (Ruderman and Kittel, 1954; Kasuya, 1956; Yosida, 1957) magnetic interaction,

$$H_{\mathrm{RKKY}} = \overbrace{-J^2\chi(\mathbf{x}-\mathbf{x}')}^{J_{\mathrm{RKKY}}(\mathbf{x}-\mathbf{x}')} \vec{S}(\mathbf{x}) \cdot \vec{S}(\mathbf{x}') \tag{62}$$

where

$$J_{\mathrm{RKKY}}(r) \sim -J^2\rho \frac{\cos 2k_{\mathrm{F}} r}{k_{\mathrm{F}} r} \tag{63}$$

In alloys containing a dilute concentration of magnetic transition-metal ions, the oscillatory RKKY interaction gives rise to a frustrated, glassy magnetic state known as a *spin glass*. In dense systems, the RKKY interaction typically gives rise to an ordered antiferromagnetic state with a Néel temperature T_{N} of the order $J^2\rho$. Heavy-electron metals narrowly escape this fate.

Doniach argued that there are two scales in the Kondo lattice, the single-ion Kondo temperature T_{K} and T_{RKKY}, given by

$$\begin{aligned} T_{\mathrm{K}} &= D\mathrm{e}^{-1/(2J\rho)} \\ T_{\mathrm{RKKY}} &= J^2\rho \end{aligned} \tag{64}$$

When $J\rho$ is small, then T_{RKKY} is the largest scale and an antiferromagnetic state is formed, but, when the $J\rho$ is large, the Kondo temperature is the largest scale so a dense Kondo lattice ground state becomes stable. In this paramagnetic state, each site resonantly scatters electrons with a phase shift $\sim\pi/2$. Bloch's theorem then insures that the resonant elastic scattering at each site acts coherently, forming a renormalized band of width $\sim T_{\mathrm{K}}$ (Figure 15).

As in the impurity model, one can identify the Kondo lattice ground state with the large U limit of the Anderson lattice model. By appealing to adiabaticity, one can then link the excitations to the small U Anderson lattice model. According to this line of argument, the quasiparticle Fermi surface volume must count the number of conduction and f electrons (Martin, 1982), even in the large U limit, where it corresponds to the number of electrons *plus* the number of spins

$$2\frac{\mathcal{V}_{\mathrm{FS}}}{(2\pi)^3} = n_e + n_{\mathrm{spins}} \tag{65}$$

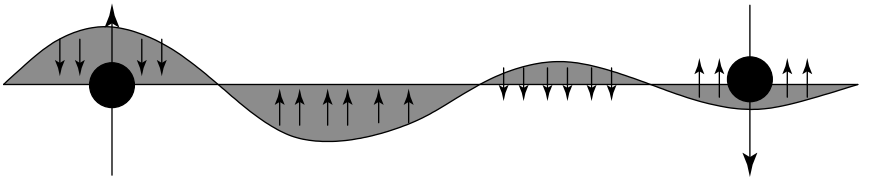

Figure 14. Spin polarization around magnetic impurity contains Friedel oscillations and induces an RKKY interaction between the spins.

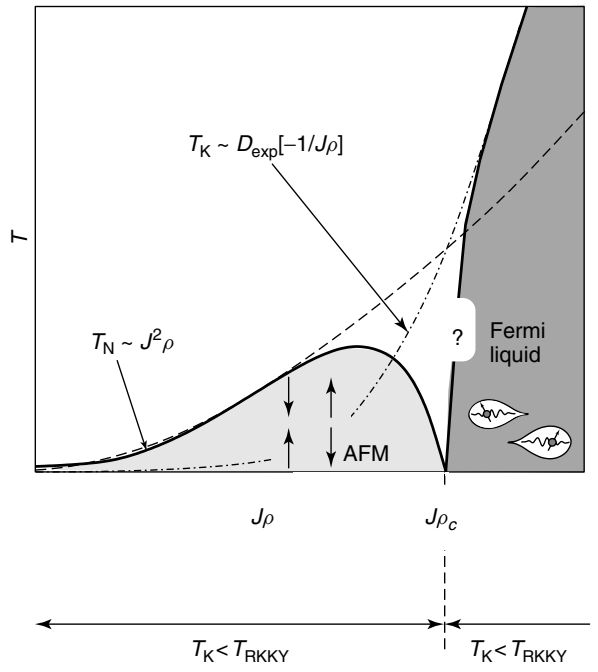

Figure 15. Doniach diagram, illustrating the antiferromagnetic regime, where $T_K < T_{RKKY}$ and the heavy-fermion regime, where $T_K > T_{RKKY}$. Experiment has told us in recent times that the transition between these two regimes is a quantum critical point. The effective Fermi temperature of the heavy Fermi liquid is indicated as a solid line. Circumstantial experimental evidence suggests that this scale drops to zero at the antiferromagnetic quantum critical point, but this is still a matter of controversy.

Using topology, and certain basic assumptions about the response of a Fermi liquid to a flux, Oshikawa (2000) was able to short circuit this tortuous path of reasoning, proving that the Luttinger relationship holds for the Kondo lattice model without reference to its finite U origins.

There are, however, aspects to the Doniach argument that leave cause for concern:

- It is purely a comparison of energy scales and does not provide a detailed mechanism connecting the heavy-fermion phase to the local moment AFM.
- Simple estimates of the value of $J\rho$ required for heavy-electron behavior give an artificially large value of the coupling constant $J\rho \sim 1$. This issue was later resolved by the observation that large spin degeneracy $2j + 1$ of the spin-orbit coupled moments, which can be as large as $N = 8$ in Yb materials, enhances the rate of scaling to strong coupling, leading to a Kondo temperature (Coleman, 1983)

$$T_K = D(NJ\rho)^{\frac{1}{N}} \exp\left[-\frac{1}{NJ\rho}\right] \tag{66}$$

Since the scaling enhancement effect stretches out across decades of energy, it is largely robust against crystal fields (Mekata *et al*., 1986).

- Nozières' exhaustion paradox (Nozières, 1985). If one considers each local moment to be magnetically screened by a cloud of low-energy electrons within an energy T_K of the Fermi energy, one arrives at an 'exhaustion paradox'. In this interpretation, the number of electrons available to screen each local moment is of the order $T_K/D \ll 1$ per unit cell. Once the concentration of magnetic impurities exceeds $\frac{T_K}{D} \sim 0.1\%$ for ($T_K = 10\,\mathrm{K}$, $D = 10^4\,\mathrm{K}$), the supply of screening electrons would be exhausted, logically excluding any sort of dense Kondo effect. Experimentally, features of single-ion Kondo behavior persist to much higher densities. The resolution to the exhaustion paradox lies in the more modern perception that spin screening of local moments extends *up* in energy, from the Kondo scale T_K out to the bandwidth. In this respect, Kondo screening is reminiscent of Cooper pair formation, which involves electron states that extend upward from the gap energy to the Debye cutoff. From this perspective, the Kondo length scale $\xi \sim v_F/T_K$ is analogous to the coherence length of a superconductor (Burdin, Georges and Grempel, 2000), defining the length scale over which the conduction spin and local moment magnetization are coherent without setting any limit on the degree to which the correlation clouds can overlap (Figure 16).